



## Energy and carbon footprint of metals through physical allocation. Implications for energy transition

Jorge Torrubia<sup>\*</sup>, Alicia Valero, Antonio Valero

Research Centre for Energy Resources and Consumption (CIRCE Institute), University of Zaragoza, CIRCE Building – Campus Río Ebro, Mariano Esquillor Gómez, 15, 50018, Zaragoza, Spain

### ARTICLE INFO

#### Keywords:

Energy footprint  
Carbon footprint  
Metals  
Life cycle inventories  
Physical allocation  
Energy transition

### ABSTRACT

The increasing metal demand driven by energy and digital transition has led to more complex mining operations. To allocate environmental impacts in cases of mining co-production, this study proposes a physical method based on the relative geological scarcity of elements, which provides the basis for an exergy cost allocation. It focuses on calculating the energy and carbon footprint of 51 metals, including 28 co-products, based on available databases. The analysis considers the fuel type, main production stages and the energy footprint of up to 25 chemicals. This study provides new insights into 39 infrequently studied metals. Results show that by using renewable electricity in production, 41 metals can reduce their carbon footprint by up to 50 %. However, key metals such as Fe or Li require additional decarbonization efforts beyond electricity. Only by decarbonizing metal production is possible a renewable infrastructure that can achieve the energy transition goals.

### 1. Introduction

The quantity and diversity of metals extracted and used by our civilization has increased steadily since the beginning of the industrial revolution. While a century ago, the diversity of metals employed was limited to about a dozen, and were mainly used for infrastructure and durable goods, 21st-century industrial societies utilize virtually the entire periodic table (Nuss and Eckelman, 2014). With the increasing demand of metals for low-carbon technologies, the concern about raw material extraction sustainability has grown (Sanjuan-Delmás et al., 2022). Mining and metal production are one of the most energy-intensive industries worldwide. It consumes about 38 % of global industrial energy use, 15 % of the global electricity use, and 11 % of global energy use. This consumption is still based on fossil fuels since it comprises about 19 % of global coal and coal products, 5 % of global gas, and 2 % of global oil supplied (Igogo et al., 2021).

On the other hand, the mining and metallurgical industries are the source of raw materials for the manufacturing, transportation, construction, and energy sectors, and, therefore, for the energy transition infrastructures. Renewable energy technologies contain various metals with specific functionalities (Bartie et al., 2022), such as REE for the permanent magnets of wind turbines, silicon and silver for the photovoltaic panels or lithium and cobalt for batteries. Herein lies one of the

keys to the energy transition, as its infrastructures will be as low-carbon as the raw materials used to manufacture them.

The study of environmental evaluation in metal production is gaining interest. Recently, some authors carried out a systematic review of existing literature (Rachid et al., 2023). On the other hand, Nuss and Eckelman (2014) conducted a comprehensive life cycle comparison of 63 metals. Other works have focused on specific metals, covering a significant percentage of global production, such as Van Genderen et al. (2016) which covers 30 % of the global zinc production; Mistry et al. (2016), 50 % of global nickel; Dolganova et al. (2020), 80 % of ferro-niobium or Schenker et al. (2022), 70 % of lithium from brines. Other authors focused on specific countries, highlighting China: Zhang et al. (2016), aluminum; Ma et al. (2017), tungsten carbide; Qi et al. (2017), zinc from hydrometallurgy; Chen et al. (2018), gold, lead, and zinc; Lu et al. (2018), tungsten; Yang et al. (2019), aluminum; Zhang et al. (2020), manganese or Bai et al. (2022), nickel. Finally, several studies identified energy-intense or high carbon footprint metals and proposed measures for their decarbonization, such as Farjana et al. (2019), Igogo et al. (2021), Norgate and Jahanshahi (2011), van der Meide et al. (2022) or Strezov et al. (2021).

However, mining and metal production involve interconnected processes with multiple co-produced metals (Nuss and Eckelman, 2014). Therefore, life cycle assessments (LCA) require methods to allocate

<sup>\*</sup> Corresponding author.

E-mail address: [jtorrubia@unizar.es](mailto:jtorrubia@unizar.es) (J. Torrubia).

<https://doi.org/10.1016/j.resconrec.2023.107281>

Received 26 June 2023; Received in revised form 9 October 2023; Accepted 19 October 2023

Available online 25 October 2023

0921-3449/© 2023 The Author(s). Published by Elsevier B.V. This is an open access article under the CC BY license (<http://creativecommons.org/licenses/by/4.0/>).

environmental impacts among these metals. For instance, ISO 14044 provides four allocation principles for co-products, which should be considered in order. The first two principles involve avoiding allocation by (1) subdividing processes or (2) expanding the system to provide co-product credits (Van Genderen et al., 2016; Mistry et al., 2016). Nevertheless, these are challenging to apply in metal production since it is impossible to identify an alternative production route in shared processes (Santero and Hendry, 2016). The remaining principles concern allocation, based (3) firstly on physical relationships (e.g., mass) and (4) lastly on any other relationship such as economic. Thus, the economic allocation is the least preferred, although is the most widespread (Farjana et al., 2019; Lai et al., 2021). For this reason, controversy persists over the use of prices (Santero and Hendry, 2016; Sonderegger et al., 2020; Schrijvers et al., 2016), as social valuations are used to determine the physical impacts involving relationships with nature. To address this issue, other authors explored alternative methodologies, such as Valero et al. (2015), using the exergy cost. It represents the cumulative exergy consumption needed to manufacture a product when the boundaries of the production, a reference environment and the exergy efficiency of each process have been defined (Valero et al., 1986). However, a challenge arises when applying allocation to metal production due to the inability to determine the exergy cost in these shared processes. Therefore, another physical feature of metals is required to avoid using prices. In this context, the relative geological scarcity of elements in the Earth's crust is selected as a first approximation. This methodology was initially introduced by Tuusjärvi et al. (2012), but their focus was limited to four mines and eight metals.

The main novelty of this paper lies in the estimation of the energy and carbon footprint of 51 metals, using solely physical parameters to allocate the footprint of the 28 co-produced metals. With this paper, we approach the rigorous evaluation of the physical (exergetic) cost formation process of all metals. We avoid the use of market prices for cost allocation, as they are inherently linked to the current historical context, and other distortions arising from monopoly, taxation, currency value and speculation. Therefore, the cost allocation of physical processes

should not be contaminated by prices. In this way, the energy footprint is also disaggregated by fuel type, which is indispensable for the future calculation of the exergy cost, and by the production stages to discuss the possibilities for decarbonization of the metal industry and its implications for the energy transition.

## 2. Data and methodology

The methodology for calculating the allocation factor and the energy footprint is described first, followed by the carbon footprint explanation.

### 2.1. Energy footprint calculation and physical allocation

The physical allocation method was applied to 28 co-products among 51 analyzed metals, being the main metal so-called the *host metal* and the others *companion metals* (Nassar et al., 2015). For instance, in Pb–Zn mines, Cd, Ag and In are companion metals. Fig. 1 shows the example of the production of these metals to understand the allocation method. It illustrates that the studied processes follow a cradle-to-gate perspective, since the mining industry supplies materials for downstream sectors and does not provide end-user products (Sanjuan-Delmás et al., 2022; Santero and Hendry, 2016). Thus, metals may become embedded in many products, drastically influencing the metal's impact during its lifetime and the reusability or recyclability at end-of-life stages.

The allocation factors (highlighted in bold in Fig. 1) were calculated using the metal production per mass of rock mined  $M_j$ , and the average elemental concentration of the metal in the Earth's crust  $CC_j$ , obtained from (Mindat.org 2023). Table 1 illustrates the example for Pb–Zn mines, indicating  $M_j$  per kilogram of rock, the corresponding elemental concentration ( $CC_j$ ), and the division between these parameters ( $CC_j^{-1} \cdot M_j$ ) for each metal mined. This division represents the concentration of each metal in the mine compared to the Earth's crust, so-called *metal mine concentration*. The allocation factors were determined by dividing the *metal mine concentration* of each metal by the *metal mine concentration* of all metals, as shown Eq. 1. (Santero and Hendry, 2016)

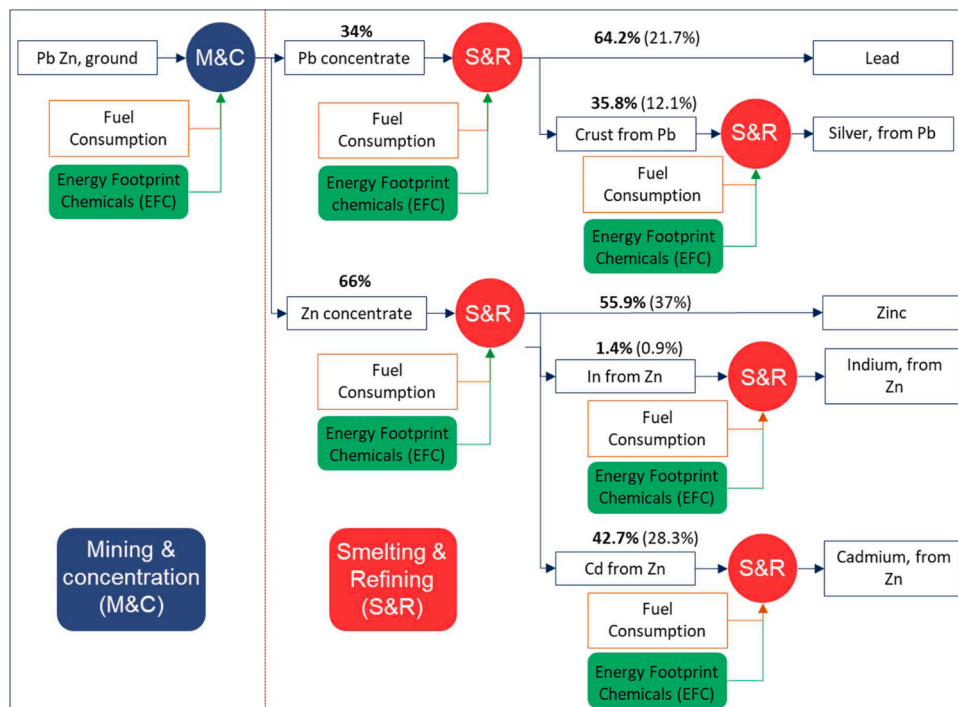


Fig. 1. Example of allocation factors and energy footprint calculations in Pb–Zn mines. The mining and concentration (M&C) stage is highlighted in blue; the smelting & refining (S&R) in red and the energy footprint of chemicals (EFC) in green. Fuel consumption includes natural gas, diesel, coal and electricity consumption. Numbers in brackets represent the allocation factor calculated in Table 1.

**Table 1**  
Data for allocation factor calculation in Pb–Zn mines.

Metal production ( $M_j$ )	Crustal concentration ( $CC_j$ )	Metal mine concentration $CC_j^{-1} \cdot M_j$	Allocation factor
kg-elem/kg-rock	kg-elem/kg-crust	kg-crust/kg-rock	%
Zn 5.48E-01	7.10E-05	7.72E+03	37.0 %
Pb 9.10E-02	2.00E-05	4.53E+03	21.7 %
Cd 5.80E-04	9.80E-08	5.91E+03	28.3 %
Ag 1.30E-04	5.00E-08	2.53E+03	12.1 %
In 9.60E-06	5.00E-08	1.91E+02	0.9 %

Once the allocation of each metal was calculated, the allocation of each process was derived, as shown in Fig. 1. For instance, the combined contributions of Zn (37 %), In (0.9 %) and Cd (28.3 %) make up the 66 % allocation of Zn concentrate. The final contributions of Zn (55.9 %), In (1.4 %) and Cd (42.7 %) were calculated in relation to the Zn concentrate stage, which represents 100 %.

$$Allocation\ factor_j\ (\%) = \frac{CC_j^{-1} \cdot M_j}{\sum_{j=1}^m (CC_j^{-1} \cdot M_j)} \quad (1)$$

Once allocation factors were determined, the energy footprint of the 28 co-produced metals was calculated. First, the fuels consumed in each process  $i$  were normalized per kilogram of metal (represented as  $EF_{Coal_i}$  in Eq. (2), for the case of coal). Thus, the energy footprint of process  $i$  ( $EF_{Coal_i}$ ) until a shared process  $X$  was determined by summing the energy footprint of a specific fuel multiplied by the allocation factor of the metal in the process  $X$  ( $AF_X$ ) Eq. (2)). Once the energy footprint of shared processes ( $EF_{Coal_x}$ ) were known, the total energy footprint of a fuel ( $EF_{Coal}$ ) was the sum of the share processes ( $EF_{Coal_x}$ ) and non-share processes ( $EF_{Coal_i}$ ), calculated using Eq. (3). For non-co-coproduct metals (23 cases) the calculation was simpler as no allocation was required, so  $EF_{Coal_x}$  was zero. Eqs. (2) and (3) only refers to coal, but the same process was applied to calculate the energy footprint of the other fuels: natural gas, diesel and electricity ( $EF_{NaturalGas}$ , for example). Once the energy footprint was calculated for all fuels, the total *Energy Footprint* was determined using Eq. (4).

$$EF_{Coal_x} = \sum_{i=1}^X EF_{Coal_i} \cdot AF_X \quad (2)$$

$$EF_{Coal} = \sum_{i=1}^n EF_{Coal_i} + EF_{Coal_x} \quad (3)$$

$$Energy\ Footprint = EF_{NaturalGas} + EF_{Diesel} + EF_{Coal} + EF_{Electricity} \quad (4)$$

Eqs. (2)–(4) calculate the total footprint considering all processes. However, the processes were categorized into three types: Mining and Concentration (M&C), Smelting and Refining (S&R), and the Energy Footprint embedded in Chemicals (EFC), as is highlighted in Fig. 1. EFC represents the energy requirement to produce a chemical that will subsequently be utilized in producing metals. This study considered up to 25 chemicals, such as ammonia, hydrochloric acid, limestone, oxygen, phosphoric acid, quicklime, soda ash or sulfuric acid. The Ecoinvent 3.9.1 database (2022) (<https://ecoinvent.org/Ecoinvent>, 2023),

**Table 2**  
Emission factors for high emission scenario (HES) and low emission scenario (LES). HES is based on the global electricity mix in 2017 (Pinto et al., 2023) and LES is based on the decarbonized mix of the reference (Jacobson et al., 2017). More information is available in the supplementary materials.

		Emission factor HES	Emission factor LES	Source
Natural gas	kgCO <sub>2</sub> eq/MJ	0.057	0.057	(Fossil Fuels Emission Factors, 2023)
Diesel	kgCO <sub>2</sub> eq/MJ	0.075	0.075	(Fossil Fuels Emission Factors, 2023)
Coal	kgCO <sub>2</sub> eq/MJ	0.1	0.1	(Fossil Fuels Emission Factors, 2023)
Electricity	kgCO <sub>2</sub> eq/kWh	0.568	0.026	(Schlömer et al., 2014; REN21 2022)

specifically the Global cases, was the primary source for LCI data for metals and chemicals. Additional references were used for Rare Earth Elements (REE) (Torrubia et al., 2022). In summary, the energy footprint was divided into four fuel types and three main contributions.

### 2.2. Carbon footprint calculation

The carbon footprint of metals was determined by considering the energy footprint and the emission factors for the different fuels, shown in Table 2. Two scenarios were considered for electricity emissions: one with high emissions (HES), based mostly on fossil fuels, and another with low emissions (LES), utilizing a combination of renewable energy sources. However, these scenarios are only indicative since electricity generation can vary significantly, emphasizing the need for further research studies.

Eq. (5) was utilized to calculate the carbon footprint of each fuel.  $EmFac$  represents the emission factor of each fuel,  $EF_{Coal_i}$  the energy footprint of each fuel in process  $i$ , and  $CF_{Coal}$  the carbon footprint produced by each fuel (in this case coal). Finally, the total carbon footprint was determined using Eq. (6), which added the contributions from the four fuels.

$$CF_{Coal} = \sum_{i=1}^n EF_{Coal_i} \cdot EmFac_{Coal} \quad (5)$$

$$Carbon\ Footprint = CF_{NaturalGas} + CF_{Diesel} + CF_{Coal} + CF_{Electricity} \quad (6)$$

Regarding the sensibility of the model, Eqs. (2)–(6) describe a linear model without feedbacks, so the error transmission is also linear. This means that no perturbations larger than the error assumed in the sensitivity analysis would be expected, as demonstrated in similar models (Font de Mora Rullán et al., 2013).

### 3. Results and discussion

This section first presents the energy footprint results using the physical allocation, comparing them with existing literature. Next, the energy footprint is analyzed by fuel type, exploring opportunities for carbon footprint reduction and discussing the implications for the energy transition.

#### 3.1. Energy footprint with a physical allocation

Table 3 shows the energy footprint results for all the studied metals in "This Study" column, ordered by atomic number (At. No.). Co-product metals are highlighted in bold, with the "host" column indicating their *host metal*. Additionally, the other columns represent the mean, minimum (min), maximum (max), standard deviation (SD) and number of samples from the references. The allocation method only applies to co-produced metals. Moreover, it is important to note that due to the complexity of mining, the same metal can originate from different deposit types. For instance, nickel can be obtained from both lateritic and sulfide ores or cobalt can be a co-product of both nickel and copper. Ecoinvent Global production LCIs were utilized to address this complexity, which generally represents the largest metal producers.

The non-co-product metals (not bolded in Table 3) should have comparable energy footprints to the literature, as these metals are not

**Table 3**  
Energy footprint results in MJ/kg.

At. No.	Host	This study	Mean	Min	Max	SD	Samples	References	
3	Li	–	69	89	50	125	26	9	(Nuss and Eckelman, 2014; Bai et al., 2022; Kelly et al., 2021; International Energy Agency 2023)
4	Be	–	5724	1720	1720	1720	–	1	(Nuss and Eckelman, 2014)
5	B	–	14	27	27	27	–	1	(Nuss and Eckelman, 2014)
12	Mg	–	199	19	19	19	–	1	(Nuss and Eckelman, 2014)
13	Al	–	74	171	23	263	65	17	(Nuss and Eckelman, 2014; Igogo et al., 2021; Yang et al., 2019; Norgate and Jahanshahi, 2011; International Energy Agency 2023; Espinosa et al., 2012; Nunez and Jones, 2016; Van der Voet et al., 2019; Farjana et al., 2019; Guzmán et al., 2022; Norgate et al., 2007)
14	Si	–	1396	5242	1490	9350	3039	5	(Fan et al., 2021; Muteri et al., 2020)
22	Ti	–	321	280	115	364	143	3	(Nuss and Eckelman, 2014; Igogo et al., 2021; Norgate et al., 2007)
24	Cr	–	265	62	40	83	30	2	(Nuss and Eckelman, 2014; Espinosa et al., 2012)
25	Mn	–	34	29	24	34	7	2	(Nuss and Eckelman, 2014; Van der Voet et al., 2019)
26	Fe	–	24	19	7	30	7	8	(Nuss and Eckelman, 2014; Van der Voet et al., 2019; Guzmán et al., 2022)
27	Co	Cu	156	129	29	653	170	12	(Nuss and Eckelman, 2014; van der Meide et al., 2022; International Energy Agency 2023; Guzmán et al., 2022)
28	Ni	–	145	156	36	290	68	15	(Nuss and Eckelman, 2014; Igogo et al., 2021; Mistry et al., 2016; Norgate and Jahanshahi, 2011; International Energy Agency 2023; Van der Voet et al., 2019; Guzmán et al., 2022; Wei et al., 2020)
29	Cu	–	23	58	18	168	39	20	(Nuss and Eckelman, 2014; Sanjuan-Delmás et al., 2022; Igogo et al., 2021; Norgate and Jahanshahi, 2011; International Energy Agency 2023; Van der Voet et al., 2019; Guzmán et al., 2022; Norgate et al., 2007)
30	Zn	Pb	19	48	36	78	12	12	(Nuss and Eckelman, 2014; Norgate and Jahanshahi, 2011; Norgate et al., 2007; Farjana et al., 2019; Farjana et al., 2019; da Silva Lima et al., 2022)
31	Ga	Al	786	3030	3030	3030	–	1	(Nuss and Eckelman, 2014)
33	As	–	75	5	5	5	–	1	(Nuss and Eckelman, 2014)
34	Se	Cu	13,115	66	66	66	–	1	(Nuss and Eckelman, 2014)
38	Sr	–	27	–	–	–	–	0	–
39	Y	REE	378	295	295	295	–	1	(Nuss and Eckelman, 2014)
40	Zr	–	410	13	4	29	14	3	(Nuss and Eckelman, 2014; Lundberg, 2011; Gediga et al., 2019)
41	Nb	–	75	127	82	172	63	2	(Nuss and Eckelman, 2014; Dolganova et al., 2020)
42	Mo	Cu	88	117	117	117	–	1	(Nuss and Eckelman, 2014)
45	Rh	PGM	1558,329	514,500	346,000	683,000	238,295	2	(Nuss and Eckelman, 2014; International Platinum Group Metals Association 2013)
46	Pd	PGM	122,789	188,350	72,700	304,000	163,554	2	(Nuss and Eckelman, 2014; International Platinum Group Metals Association 2013)
47	Ag	Pb–Zn, Cu, Au	11,246	1745	210	3280	2171	2	(Nuss and Eckelman, 2014; Espinosa et al., 2012)
48	Cd	Zn	14,171	53	53	53	–	1	(Nuss and Eckelman, 2014)
49	In	Zn	27,716	1720	1720	1720	–	1	(Nuss and Eckelman, 2014)
50	Sn	–	64	321	321	321	–	1	(Nuss and Eckelman, 2014)
51	Sb	–	34	141	141	141	–	1	(Nuss and Eckelman, 2014)
52	Te	Cu	217,825	435	435	435	–	1	(Nuss and Eckelman, 2014)
56	Ba	–	24	4	4	4	–	1	(Nuss and Eckelman, 2014)
57	La	REE	473	215	215	215	–	1	(Nuss and Eckelman, 2014)
58	Ce	REE	166	252	252	252	–	1	(Nuss and Eckelman, 2014)
59	Pr	REE	2240	376	376	376	–	1	(Nuss and Eckelman, 2014)
60	Nd	REE	562	161	78	244	117	2	(Nuss and Eckelman, 2014; International Energy Agency 2023)
62	Sm	REE	1092	1160	1160	1160	–	1	(Nuss and Eckelman, 2014)
63	Eu	REE	5011	7750	7750	7750	–	1	(Nuss and Eckelman, 2014)
64	Gd	REE	1354	914	914	914	–	1	(Nuss and Eckelman, 2014)
65	Tb	REE	7179	5820	5820	5820	–	1	(Nuss and Eckelman, 2014)
66	Dy	REE	1455	1170	1170	1170	–	1	(Nuss and Eckelman, 2014)
67	Ho	REE	5778	4400	4400	4400	–	1	(Nuss and Eckelman, 2014)
68	Er	REE	2123	954	954	954	–	1	(Nuss and Eckelman, 2014)
69	Tm	REE	13,132	12,700	12,700	12,700	–	1	(Nuss and Eckelman, 2014)
70	Yb	REE	2088	2450	2450	2450	–	1	(Nuss and Eckelman, 2014)
71	Lu	REE	14,184	17,600	17,600	17,600	–	1	(Nuss and Eckelman, 2014)
73	Ta	–	1195	4360	4360	4360	–	1	(Nuss and Eckelman, 2014)
74	W	–	161	133	133	133	–	1	(Nuss and Eckelman, 2014)
78	Pt	PGM	76,135	315,000	243,000	387,000	101,823	2	(Nuss and Eckelman, 2014; International Platinum Group Metals Association 2013)
79	Au	–	243,437	294,504	146,000	666,000	146,786	10	(Nuss and Eckelman, 2014; Igogo et al., 2021; Ulrich et al., 2022; Norgate and Haque, 2012)
80	Hg	–	125	179	179	179	–	1	(Nuss and Eckelman, 2014)
82	Pb	Zn	10	25	19	32	6	8	(Nuss and Eckelman, 2014; Igogo et al., 2021; Norgate and Jahanshahi, 2011; Van der Voet et al., 2019; Norgate et al., 2007)

affected by the allocation method used. However, only seven metals (Li, Al, Si, Fe, Ni, Cu and Au) have sufficient literature samples (>3) for comparison. These results align with the literature, except for Si, which closely approaches to the minimum reported (1396 vs 1490 MJ/kg). This confirms that the LCI used for these elements is comparable with

the literature.

On the other hand, other metals differ considerably from the literature, such as Be, Mg, Cr, As and Zr. These differences can be attributed to the utilization of different LCI. However, the limited availability of samples hampers comprehensive comparison. Only 1 or 2 references

have been found for 39 metals. Therefore, this study also provides more information on many under-researched but indispensable metals for the energy and digital transition (Torrubia et al., 2022; Torrubia et al., 2023).

Comparing the energy footprint of co-product metals was also challenging due to limited literature studies. Exceptions include Co, Pb, and Zn (with more than six samples), which show results comparable to the literature. However, greater differences exist for other co-products like Se, Te, In and Cd. In these cases, the variations observed could be attributed to utilizing distinct allocation systems. However, the physical allocation system used in this study offers several advantages over the economic approach used in these last cases. Firstly, it presents more consistent and stable results over time than the economic allocation, as it only depends on metal production (as shown in Eq. (1)) and is unaffected by price fluctuations. This stability is particularly crucial in the context of price volatility caused by factors like pandemics, conflicts and speculation. Secondly, the energy and carbon footprint are indicators of physical impacts, so they should be determined only through physical parameters. There is a clear distinction between price, which arises from social relationships of a specific historical moment, and physical environmental impacts, which emerge from our permanent relationship with nature. Consequently, the use of economic allocation, which combines social valuations with physical impacts (energy/carbon footprint) is not

consistent. Thirdly, the proposed allocation method considers the inherent physical value of metals based on their natural abundance or scarcity on Earth's crust, assuming that scarce metals are more costly. Additionally, this is an undeniable truth, as the relative scarcity of elements in the Earth's crust can hardly be altered.

Finally, this approach establishes the basis for exergy cost allocation. A second iteration could estimate the exergy cost from the energy footprint. The Current Exergy Cost (CEC) of metals, representing the exergy cost from current mines to refined metals, could be expanded to include the Exergy Replacement Cost (ERC). This addition extends the study to a cradle-to-grave perspective, encompassing the exergy cost of concentrating minerals from a dispersed state, the so-called Thanatia, to current mines (Torrubia et al., 2022; Valero and Valero, 2014). Therefore, the sum of CEC and ERC represents thermodynamic rarity (TR) (Torrubia et al., 2022). Thus, CEC, ERC, and TR can be calculated more robustly by following this methodology. This approach will be further explored in future studies.

### 3.2. Energy footprint by fuel type consumption

Fig. 2 shows the energy footprint results ordered from highest to lowest value in MJ/kg. The footprint is divided into four fuels (natural gas, diesel, coal and electricity) and three parts: M&C, S&R and EFC, as

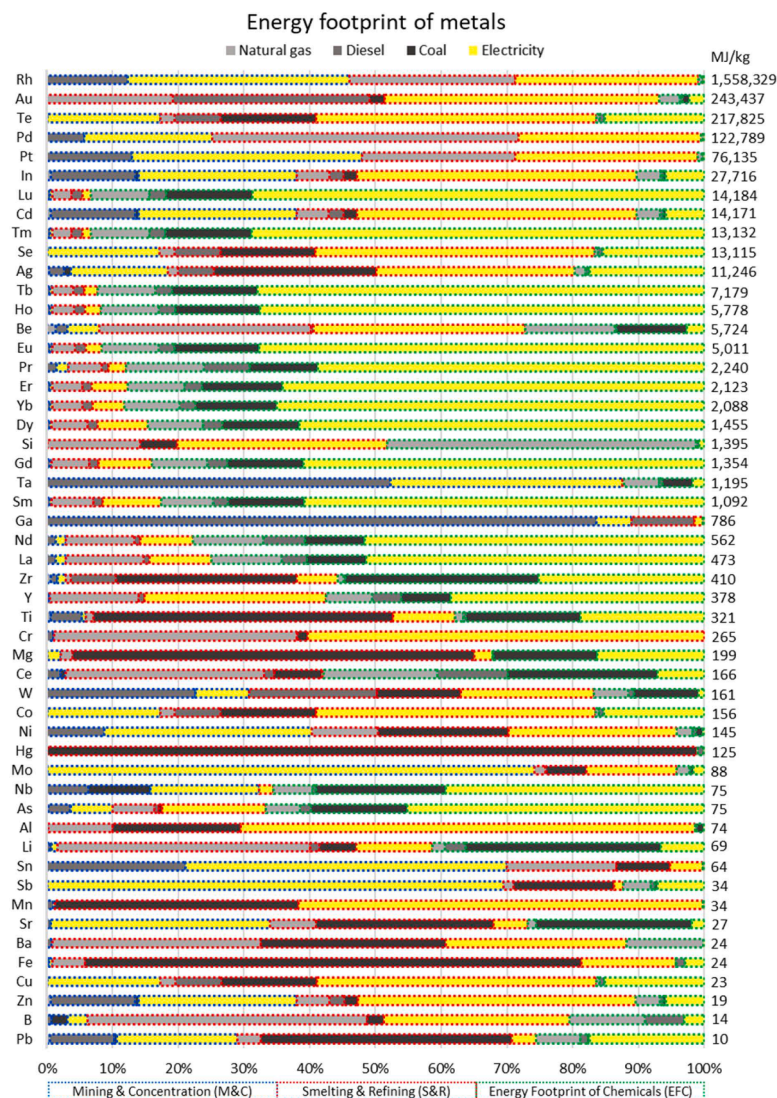


Fig. 2. Energy footprint results by fuel type. The blue box indicates the energy footprint of mining and concentration(M&C); the red box of smelting and refining (S&R) and the green box the energy footprint of chemicals (EFC).

indicated in Section 2.1.

### 3.2.1. Mining and concentration processes

M&C processes include all the processes from rock extraction to the production of a mineral concentrate. Fig. 2 shows the energy footprint of these processes with a blue bar. The figure illustrates that the total contribution of this stage to the energy footprint is lower than the contribution of S&R in most cases. For 43 metals, the M&C contribution is below 40 %, while only 5 metals (Ga, Ta, Sb, Mo and Sn) have a M&C contribution exceeding 50 %. All these metals exhibit a low EFC, potentially caused by an underestimation due to insufficient data in the LCI, which would increase the M&C contribution. Additionally, mercury and gold present a 100 % M&C contribution, since LCI data for S&R stage were unavailable.

These results are consistent with the literature, as Norgate et al. (Norgate and Jahanshahi, 2011) stated: “Mineral processing & concentration, usually have much less impact than metal extraction and refining in terms of energy”. Although this stage contributes less to the total energy footprint, several studies argue that this share could increase in the future due to the declining ore grades and more complex ores (Norgate and Jahanshahi, 2011; Norgate et al., 2007; Norgate and Haque, 2012; Norgate and Haque, 2010; Calvo et al., 2016). Therefore, decarbonization measures are also required at the M&C stage to decouple the energy consumption from the carbon footprint.

The fuel used is a key factor in this decoupling, as not all fuels are equally replaceable with low-carbon alternatives. Fig. 2 shows that diesel and electricity are the main fuels of M&C, contributing 70 % at this stage. Igogo et al. (2021), reported similar results, with 33 % of mining energy came from diesel and 40 % from electricity. The use of diesel in mining machinery is predominant, especially in trucks. Sanjuan-Delmás et al. (2022), found that 99 % of fossil fuel consumption in a Swedish mine was attributed to diesel in trucks. However, reducing diesel consumption in trucks is a challenge. Electric or fuel cell vehicles have been proposed (Sanjuan-Delmás et al., 2022; Ulrich et al., 2022), but their implementation in mining operations remains limited (Anglo-American Press releases, 2023).

Electricity in M&C is mainly used for comminution and HVAC systems in underground mines. For instance, comminution accounts for 15 % and 21 % of the energy demand in iron and gold production, respectively (Ulrich et al., 2022; Ferreira and Leite, 2015). Decarbonizing M&C electricity use faces challenges in integrating renewables in remote off-grid operations, although the number of projects is increasing (from 600 MW in 2015 to 5 GW in 2019). However, this renewable capacity remains a fraction of the total energy demand, indicating slow progress (Igogo et al., 2021). Increasing the share of renewables in the grid for connected mining operations is another challenge. Nevertheless, electrified processes are easier to decarbonize than diesel consumption (Ulrich et al., 2022).

### 3.2.2. Smelting and refining processes

S&R processes transform ore concentrate into metallic form. Fig. 2 illustrates S&R energy footprint with a red bar, showing their high energy footprint contribution, which is supported by other studies (Nuss and Eckelman, 2014; Hamuyuni et al., 2022). Thus, S&R accounts for the majority of fossil fuel usage of the total energy, surpassing diesel consumption during M&C. For instance, in 40 metals, over 75 % of fossil fuel consumption occurs during S&R.

Natural gas and coal are the main fuels used in S&R stage, accounting for over 70 % of fossil fuel consumption in 42 metals. These fuels provide heat and serve as reductants. Promising alternatives include bioreducers and hydrogen (Hamuyuni et al., 2022). However, bioreductants like charcoal could present alternative problems, including their global-scale sustainable production or technical issues due to their physical properties (Igogo et al., 2021). On the other hand, hydrogen has a better environmental impact when produced using renewable electricity. However, its high cost and the need for new infrastructure remain

challenging (Nicoletti et al., 2015).

### 3.2.3. Energy footprint of chemicals

Fig. 2 shows the contribution of EFC with a green bar. Chemicals play a significant role in S&R processes, with less involvement in M&C processes. In 19 out of 51 metals studied, EFC accounts for at least 50 % of the energy footprint. Notably, all 15 REE analyzed have an EFC exceeding 50 %, ranging from 57 % for Yttrium to 93 % of Thullium or Lutetium. This higher chemical requirement for separation can be explained due to the similar chemical properties of REE, which use processes such as solvent extraction (Torrubia et al., 2022). Another remarkable example is lithium, where 40 % of the energy footprint is attributed to EFC, mainly due to the intensive use of quicklime. Decarbonizing the production of quicklime poses challenges as it heavily relies on fossil fuels and generates CO<sub>2</sub> as waste.

These cases highlight the interdependence between industries, indicating that decarbonization efforts in mining and metal production should be extended to other industries, such as the chemical. Thus, it underlines the interconnected nature of the industrial sectors and the need of the joint decarbonization of them.

### 3.3. Carbon footprint analysis and its implications in the energy transition

The previous section emphasized the challenge of substituting fossil fuels with electricity. Furthermore, Fig. 2 highlights the significant role of electricity in the energy footprint, with 16 metals accounting for over 50 % and 24 elements up to 30 %. Two emissions scenarios for electricity generation, HES and LES, were established as described in the Methodology. Table 4 shows the results of these scenarios and compares them with others in the literature.

Table 4 includes the same columns as Table 3, with the addition of the “HES”, “LES” and “Diff (%)” columns. The “Diff (%)” column indicates the percentage difference between HES and LES scenarios. The incorporation of renewable sources in electricity generation (LES scenario) leads to significant reductions in the carbon footprint: over 50 % for 41 metals. Other studies also highlight high carbon footprint reductions in metals, such as Cu (Sanjuan-Delmás et al., 2022), Al (Zhang et al., 2016; Nunez and Jones, 2016; Norgate et al., 2007), Ni (Van der Voet et al., 2019), Mn (Zhang et al., 2020; Farjana et al., 2019), Co (van der Meide et al., 2022; Zhang et al., 2021), Zn (Strezov et al., 2021), Au (Strezov et al., 2021) by changing the electricity source. This study aligns with those findings, showing that these metals can achieve over 68 % reduction in their carbon footprint. Thus, the electricity mix and the location of metal production plants play an important role in decarbonization since electricity is usually sourced from the grid. For instance, China’s coal-based electricity contributes to a high carbon footprint of aluminum (Nunez and Jones, 2016), while copper production in Sweden benefits from a low carbon footprint due to its highly decarbonized electricity mix (Sanjuan-Delmás et al., 2022).

However, certain metals are less influenced by changes in the electricity source. For example, the carbon footprint of Fe only decreases by 25 % in LES, which is consistent with the study (Van der Voet et al., 2019). This is attributed to the inherent emissions in the Fe production process due to the use of coke as a reductant. This represents a challenge for decarbonizing the metallurgical industry due to the large-scale production of Fe (van der Meide et al., 2022). Similarly, Li exhibits a relatively low decrease in emissions (31 %) that can be attributed to quicklime production, which has a large carbon footprint (Schenker et al., 2022; Kelly et al., 2021).

In summary, the decarbonization of electricity alone significantly decouples energy and carbon footprint for most metals. However, achieving this requires deploying renewable energies, which are highly metal-intensive (Carrara et al., 2020). It creates a feedback loop that progress over time: using renewables in mining leads to cleaner metals for future renewable infrastructure (wind turbines, photovoltaic panels, or batteries), which in turn will produce cleaner energy for a new

**Table 4**  
Carbon footprint results compared to the literature in kg CO<sub>2</sub>-eq/kg.

n°		HES	LES	Diff (%)	Mean	Min	Max	SD	Samples	REFs
3	Li	6.4	4.4	31.2 %	7	2	32	7	24	(Nuss and Eckelman, 2014; Schenker et al., 2022; Kelly et al., 2021; Guzmán et al., 2022; Manjong et al., 2021)
4	Be	583	241	58.7 %	122	122	122	–	1	(Nuss and Eckelman, 2014)
5	B	1.3	0.6	54.6 %	1.0	0.5	1.5	1	2	(Nuss and Eckelman, 2014; Türkbay et al., 2022)
12	Mg	22.1	16	28.7 %	23	5	44	14	5	(Nuss and Eckelman, 2014; Angel, 2016; Ehrenberger; Simone 2013)
13	Al	10.1	2.3	76.9 %	16	2	41	9	23	(Nuss and Eckelman, 2014; Igogo et al., 2021; Zhang et al., 2016; Yang et al., 2019; Farjana et al., 2019; Nunez and Jones, 2016; Van der Voet et al., 2019; Farjana et al., 2019; Guzmán et al., 2022; Norgate et al., 2007; Manjong et al., 2021; Farjana et al., 2019)
14	Si	128.8	60	53.4 %	461	114	775	238	5	(Fan et al., 2021; Muteri et al., 2020)
22	Ti	36.6	23	38.3 %	27	8	36	16	3	(Nuss and Eckelman, 2014; Igogo et al., 2021; Norgate et al., 2007)
24	Cr	31.4	7.3	76.7 %	2.4	2.4	2.4	–	1	(Nuss and Eckelman, 2014)
25	Mn	4.5	1.4	68.9 %	5.2	1.0	9.6	3	10	(Nuss and Eckelman, 2014; Zhang et al., 2020; Van der Voet et al., 2019; Farjana et al., 2019; Manjong et al., 2021)
26	Fe	2.5	1.9	24.9 %	3.9	1.2	23.3	7	11	(Nuss and Eckelman, 2014; Van der Voet et al., 2019; Guzmán et al., 2022; Ferreira and Leite, 2015)
27	Co	20.5	6.4	68.6 %	14	4	38	12	11	(Nuss and Eckelman, 2014; Sanjuan-Delmás et al., 2022; Guzmán et al., 2022; Farjana et al., 2019; Zhang et al., 2021)
28	Ni	18.1	5.6	68.9 %	13	7	27	5	26	(Nuss and Eckelman, 2014; Igogo et al., 2021; Mistry et al., 2016; Bai et al., 2022; Strezov et al., 2021; Van der Voet et al., 2019; Guzmán et al., 2022; Norgate et al., 2007; Wei et al., 2020; Manjong et al., 2021; Farjana et al., 2019)
29	Cu	3.2	0.6	80.5 %	5.5	1.1	64.9	9	46	(Nuss and Eckelman, 2014; Sanjuan-Delmás et al., 2022; Igogo et al., 2021; Strezov et al., 2021; Tuusjärvi et al., 2012; Van der Voet et al., 2019; Guzmán et al., 2022; Norgate et al., 2007; Manjong et al., 2021; Farjana et al., 2019)
30	Zn	2.6	0.5	81.3 %	4.1	2.7	6.1	1	15	(Nuss and Eckelman, 2014; Zhang et al., 2016; Strezov et al., 2021; Norgate et al., 2007; Farjana et al., 2019; Farjana et al., 2019; da Silva Lima et al., 2022; Ehrenberger; Simone 2013; Farjana et al., 2019)
31	Ga	63.4	55.5	12.4 %	205	205	205	–	1	(Nuss and Eckelman, 2014)
33	As	9.9	2.3	76.6 %	0.3	0.3	0.3	–	1	(Nuss and Eckelman, 2014)
34	Se	1839	358	80.5 %	3.6	3.6	3.6	–	1	(Nuss and Eckelman, 2014)
38	Sr	3.2	1.6	51.1 %	3.2	3.2	3.2	–	1	(Nuss and Eckelman, 2014)
39	Y	49	10.6	78.1 %	–	–	–	–	0	–
40	Zr	47	27.2	42.6 %	3.4	0.1	15.1	7	5	(Nuss and Eckelman, 2014; Tuusjärvi et al., 2012; Lundberg, 2011; Gediga et al., 2019)
41	Nb	9.7	3.1	67.7 %	8.4	5.1	12.5	4	3	(Nuss and Eckelman, 2014; Dolganova et al., 2020; Guzmán et al., 2022)
42	Mo	13.3	1.3	89.9 %	12	6	24	8	4	(Nuss and Eckelman, 2014; Tuusjärvi et al., 2012)
45	Rh	189,139	44,304	76.6 %	40,794	14,948	78,386	23,731	5	(Nuss and Eckelman, 2014; Tuusjärvi et al., 2012; International Platinum Group Metals Association 2013)
46	Pd	12,971	4204	67.6 %	15,128	3880	28,747	11,049	5	(Nuss and Eckelman, 2014; Tuusjärvi et al., 2012; International Platinum Group Metals Association 2013)
47	Ag	1489	432	71.0 %	283	34	815	301	10	(Nuss and Eckelman, 2014; Farjana et al., 2019; Tuusjärvi et al., 2012; Farjana et al., 2019)
48	Cd	1898	354	81.4 %	3	3	3	–	1	(Nuss and Eckelman, 2014)
49	In	3713	692	81.4 %	102	102	102	–	1	(Nuss and Eckelman, 2014)
50	Sn	7.6	2.4	68.4 %	17	17	17	–	1	(Nuss and Eckelman, 2014)
51	Sb	5.3	0.9	82.6 %	13	13	13	–	1	(Nuss and Eckelman, 2014)
52	Te	30,547	5933	80.6 %	22	22	22	–	1	(Nuss and Eckelman, 2014)
56	Ba	2.3	1.3	42.9 %	0.2	0.2	0.2	–	1	(Nuss and Eckelman, 2014)
57	La	59	14.6	75.3 %	11	11	11	–	1	(Nuss and Eckelman, 2014)
58	Ce	13	11	14.0 %	13	13	13	–	1	(Nuss and Eckelman, 2014)
59	Pr	284	71	75.1 %	19	19	19	–	1	(Nuss and Eckelman, 2014)
60	Nd	70	18	74.4 %	18	18	18	–	1	(Nuss and Eckelman, 2014)
62	Sm	145	30	79.1 %	59	59	59	–	1	(Nuss and Eckelman, 2014)
63	Eu	673	141	79.0 %	395	395	395	–	1	(Nuss and Eckelman, 2014)
64	Gd	180	38	78.8 %	47	47	47	–	1	(Nuss and Eckelman, 2014)
65	Tb	964	203	79.0 %	297	297	297	–	1	(Nuss and Eckelman, 2014)
66	Dy	193	41	78.8 %	30	30	30	–	1	(Nuss and Eckelman, 2014)
67	Ho	775	163	78.9 %	226	226	226	–	1	(Nuss and Eckelman, 2014)
68	Er	283	60	78.8 %	49	49	49	–	1	(Nuss and Eckelman, 2014)
69	Tm	1766	371	79.0 %	649	649	649	–	1	(Nuss and Eckelman, 2014)
70	Yb	280	58	79.1 %	125	125	125	–	1	(Nuss and Eckelman, 2014)
71	Lu	1907	401	79.0 %	896	896	896	–	1	(Nuss and Eckelman, 2014)
73	Ta	127	60	53.0 %	260	260	260	–	1	(Nuss and Eckelman, 2014)
74	W	17	10	42.5 %	38	13	69	28	3	(Nuss and Eckelman, 2014; Ma et al., 2017; Lu et al., 2018)
78	Pt	9350	2124	77.3 %	27,488	12,500	34,699	8844	5	(Nuss and Eckelman, 2014; Tuusjärvi et al., 2012; International Platinum Group Metals Association 2013)
79	Au	26,337	10,191	61.3 %	29,222	2016	85,500	21,825	32	(Nuss and Eckelman, 2014; Igogo et al., 2021; Chen et al., 2018; Farjana et al., 2019; Strezov et al., 2021; Tuusjärvi et al., 2012; Ulrich et al., 2022; Norgate and Haque, 2012; Farjana et al., 2019)
80	Hg	12	12	0.3 %	12	12	12	–	1	(Nuss and Eckelman, 2014)
82	Pb	1.1	0.5	51.6 %	2	1	3	1	10	(Nuss and Eckelman, 2014; Igogo et al., 2021; Chen et al., 2018; Farjana et al., 2019; Strezov et al., 2021; Van der Voet et al., 2019; Norgate et al., 2007)

generation of cleaner metals. Nevertheless, for a complete decoupling, additional efforts must be taken to replace fossil fuels with renewables, such as green hydrogen, since switching electricity sources only reduces part of the carbon footprint, as is the case for Fe and Li.

#### 4. Conclusions

The energy footprint of the 51 metals studied was divided into the main fuels (natural gas, diesel, coal, and electricity) and three stages (M&C, S&R and EFC). This approach allowed to estimate the carbon footprint based on the emission factors of fuels. Unlike the commonly used economic allocation, this study employed a physical allocation method, which offers several advantages. First, it avoids the volatile nature of metals prices on time. Secondly, allocate physical impacts, such as energy or carbon footprint, based on the relative scarcity of elements in the Earth's crust, i.e., objective physical parameters, rather than temporary social relationships like prices. Thirdly, the premise that scarcer metals in the Earth's crust are more costly drives the allocation of the footprints. Due to the limited number of studies available, comparing the results is challenging, since only 1 or 2 references were found for 39 metals. Thus, this study provides valuable insights into metals that have received less attention in previous research. On the other hand, the estimation of the energy footprint provides the basis for a more robust exergy allocation that would allow the calculation of the Current Exergy Cost, Exergy Replacement Cost and Thermodynamic Rarity of metals.

Two emission scenarios are proposed for carbon footprint analysis: one with electricity based on fossil fuels and the other on renewable energies. Switching electricity to renewable energies sources, the carbon footprint of 41 metals is reduced by up to 50 %. The reason is the significant role of electricity, contributing over 50 % to the energy footprint in 16 metals and up to 30 % in 24 metals. However, Fe and Li only decrease their carbon footprint by 25 % and 31 %, respectively, indicating the need for further decarbonization efforts beyond renewable electricity.

Decarbonizing metals is crucial for the energy transition as these are the backbone of the new renewable means of production (wind turbines, solar panels, electrolyzers or batteries). Thus, cleaner metal production leads to cleaner subsequent generations of renewable means of production and products. Under this approach, further research is needed to fully comprehend the footprint of metals required for deploying a renewable infrastructure to achieve the goals of the energy transition.

#### CRedit authorship contribution statement

**Jorge Torrubia:** Conceptualization, Methodology, Investigation, Formal analysis, Data curation, Writing – original draft. **Alicia Valero:** Writing – review & editing, Supervision, Funding acquisition. **Antonio Valero:** Writing – review & editing, Supervision.

#### Declaration of Competing Interest

The authors declare that they have no known competing financial interests or personal relationships that could have appeared to influence the work reported in this paper.

#### Data availability

Data will be made available on request.

#### Acknowledgements

This research has received funding from: Grant TED2021-131397B-I00 funded by MCIN/AEI/ 10.13039/501100011033, and by the European Union NextGenerationEU/PRTR and Grant RESET: PID2020-

116851RB-I00 funded by MCIN/AEI/10.13039/501100011033.

#### Supplementary materials

Supplementary material associated with this article can be found, in the online version, at doi:10.1016/j.resconrec.2023.107281.

#### References

- Angel, H., 2016. *Water and Carbon Footprints of Mining and Producing Cu, Mg and Zn: A Comparative Study of Primary and Secondary Sources*. Lund University: Lund, Sweden.
- Anglo-American Press releases Anglo American unveils a prototype of the world's largest hydrogen-powered mine haul truck - a vital step towards reducing carbon emissions over time available online: <https://www.angloamerican.com/media/press-releases/2022/06-05-2022#> (accessed on 7 March 2023).
- Bai, Y., Zhang, T., Zhai, Y., Jia, Y., Ren, K., Hong, J., 2022. Strategies for improving the environmental performance of nickel production in China: insight into a life cycle assessment. *J. Environ. Manag.* 312. <https://doi.org/10.1016/j.jenvman.2022.114949>.
- Bartie, N., Cobos-Becerra, L., Fröhling, M., Schlatmann, R., Reuter, M., 2022. Metallurgical infrastructure and technology criticality: the link between photovoltaics, sustainability, and the metals industry. *Miner. Econ.* 35, 503–519. <https://doi.org/10.1007/s13563-022-00313-7>.
- Calvo, G., Mudd, G., Valero, A., Valero, A., 2016. Decreasing ore grades in global metallic mining: a theoretical issue or a global reality? *Resources* 5. <https://doi.org/10.3390/resources5040036>.
- Carrara, S., Alves Dias, P., Plazzotta, B., Pavel, C., 2020. *Raw Materials Demand For Wind and Solar PV Technologies in the Transition Towards a Decarbonised Energy System*. Publications Office of the European Union, Luxembourg, 2020; ISBN 9789276162254.
- Chen, W., Geng, Y., Hong, J., Dong, H., Cui, X., Sun, M., Zhang, Q., 2018. Life cycle assessment of gold production in China. *J. Clean. Prod.* 179, 143–150. <https://doi.org/10.1016/j.jclepro.2018.01.114>.
- da Silva Lima, L., Alvarenga, R.A.F., de Souza Amaral, T., de Tarso Gonçalves Noll, P., Dewulf, J., 2022. Life cycle assessment of ferriobium and niobium oxides: quantifying the reduction of environmental impacts as a result of production process improvements. *J. Clean. Prod.* 348 <https://doi.org/10.1016/j.jclepro.2022.131327>.
- Dolganova, I., Bosch, F., Bach, V., Baitz, M., Finkbeiner, M., 2020. Life cycle assessment of ferro niobium. *Int. J. Life Cycle Assess.* 25, 611–619. <https://doi.org/10.1007/s11367-019-01714-7>.
- Ehrenberger, Simone, 2013. Carbon footprint of magnesium production and its use in transport applications update of the IMA report. *Life Cycle Assessment of Magnesium Components in Vehicle Construction*, p. 2020.
- Espinosa, N., García-Valverde, R., Urbina, A., Lenzmann, F., Manceau, M., Angmo, D., Krebs, F.C., 2012. Life cycle assessment of ITO-free flexible polymer solar cells prepared by roll-to-roll coating and printing. In: *Proceedings of the Solar Energy Materials and Solar Cells*, 97. Elsevier B.V., pp. 3–13.
- Fan, M., Yu, Z., Ma, W., Li, L., 2021. Life cycle assessment of crystalline silicon wafers for photovoltaic power generation. *Silicon* 13, 3177–3189. <https://doi.org/10.1007/s12633-020-00670-4>/Published.
- Farjana, S.H., Huda, N., Mahmud, M.A., 2019a. Impacts of aluminum production: a cradle to gate investigation using life-cycle assessment. *Sci. Total Environ.* 663, 958–970. <https://doi.org/10.1016/j.scitotenv.2019.01.400>.
- Farjana, S.H., Huda, N., Mahmud, M.A.P., 2019b. Life cycle assessment of cobalt extraction process. *J. Sustain. Mining* 18, 150–161. <https://doi.org/10.1016/j.jsm.2019.03.002>.
- Farjana, S.H., Huda, N., Mahmud, M.A.P., Lang, C., 2019c. Impact analysis of gold and silver refining processes through life-cycle assessment. *J. Clean. Prod.* 228, 867–881. <https://doi.org/10.1016/j.jclepro.2019.04.166>.
- Farjana, S.H., Huda, N., Mahmud, M.A.P., Lang, C., 2019d. Life-cycle assessment of solar integrated mining processes: a sustainable future. *J. Clean. Prod.* 236. <https://doi.org/10.1016/j.jclepro.2019.117610>.
- Farjana, S.H., Huda, N., Mahmud, M.A.P., Lang, C., 2019e. A global life cycle assessment of manganese mining processes based on ecoinvent database. *Sci. Total Environ.* 688, 1102–1111. <https://doi.org/10.1016/j.scitotenv.2019.06.184>.
- Farjana, S.H., Huda, N., Parvez Mahmud, M.A., Saidur, R., 2019f. A review on the impact of mining and mineral processing industries through life cycle assessment. *J. Clean. Prod.* 231, 1200–1217.
- Ferreira, H., Leite, M.G.P., 2015. A life cycle assessment study of iron ore mining. *J. Clean. Prod.* 108, 1081–1091. <https://doi.org/10.1016/j.jclepro.2015.05.140>.
- Font de Mora Rullán, E., Valero Capilla, A., Torres Cuadra, C., 2013. *Application of Thermoconomics to Assess and Improve the Efficiency of Bioenergy Production Plants and Land-To-Tank Cycles*. University of Zaragoza.
- Gediga, J., Morfino, A., Finkbeiner, M., Schulz, M., Harlow, K., 2019. Life cycle assessment of zircon sand. *Int. J. Life Cycle Assess.* 24, 1976–1986. <https://doi.org/10.1007/s11367-019-01619-5>/Published.
- Guzmán, J.I., Faúndez, P., Jara, J.J., Retamal, C., 2022. On the source of metals and the environmental sustainability of battery electric vehicles versus internal combustion engine vehicles: the lithium production case study. *J. Clean. Prod.* 376. <https://doi.org/10.1016/j.jclepro.2022.133588>.
- Hamuyuni, J., Tesfaye, F., Iloje, C.O., Anderson, A.E., 2022. Energy efficiency and low carbon footprint in metals processing. *JOM* 74, 1886–1888.



- <https://ecoinvent.org/Ecoinvent Database Version 3.9.1 Available online: https://ecoinvent.org/the-ecoinvent-database/> (accessed on 7 March 2023).
- <https://ghgprotocol.org/Fossil Fuels Emission Factors Available Online: https://ghgprotocol.org/> (accessed on 7 March 2023).
- Igogo, T., Awuah-Offei, K., Newman, A., Lowder, T., Engel-Cox, J., 2021. Integrating renewable energy into mining operations: opportunities, challenges, and enabling approaches. *Appl. Energy* 300. <https://doi.org/10.1016/j.apenergy.2021.117375>.
- International Energy Agency Energy technology perspectives 2023; 2023; International Platinum Group Metals Association, 2013. *The Life Cycle Assessment of Platinum Group Metals* (PGMs).
- Jacobson, M.Z., Delucchi, M.A., Bauer, Z.A.F., Goodman, S.C., Chapman, W.E., Cameron, M.A., Bozonnat, C., Chobadi, L., Clonts, H.A., Enevoldsen, P., et al., 2017. 100% Clean and renewable wind, water, and sunlight all-sector energy roadmaps for 139 countries of the world. *Joule* 1, 108–121. <https://doi.org/10.1016/j.joule.2017.07.005>.
- Kelly, J.C., Wang, M., Dai, Q., Winjobi, O., 2021. Energy, greenhouse gas, and water life cycle analysis of lithium carbonate and lithium hydroxide monohydrate from brine and ore resources and their use in lithium ion battery cathodes and lithium ion batteries. *Resour. Conserv. Recycl.* 174. <https://doi.org/10.1016/j.resconrec.2021.105762>.
- Lai, F., Laurent, F., Beylot, A., Villeneuve, J., 2021. Solving multifunctionality in the carbon footprint assessment of primary metals production: comparison of different approaches. *Miner. Eng.* 170. <https://doi.org/10.1016/j.mineng.2021.107053>.
- Lu, K., Gong, X., Sun, B., Ding, Q., 2018. Life cycle assessment of tungsten production in China. In: *Proceedings of the Materials Science Forum*, 944 MSF. Trans Tech Publications Ltd, pp. 1137–1143.
- Lundberg, M. Environmental analysis of zirconium alloy production; 2011; Ma, X., Qi, C., Ye, L., Yang, D., Hong, J., 2017. Life cycle assessment of tungsten carbide powder production: a case study in China. *J. Clean. Prod.* 149, 936–944. <https://doi.org/10.1016/j.jclepro.2017.02.184>.
- Manjong, N.B., Usai, L., Burheim, O.S., Strømman, A.H., 2021. Life cycle modelling of extraction and processing of battery minerals—a parametric approach. *Batteries* 7. <https://doi.org/10.3390/batteries7030057>.
- Mindat.org, 2023. Element Concentration in the Earth's Crust. Available online 22/03/. <https://www.mindat.org/element/Lithium> (accessed on 22 March 2023).
- Mistry, M., Gediga, J., Boonzaier, S., 2016. Life cycle assessment of nickel products. *Int. J. Life Cycle Assess.* 21, 1559–1572. <https://doi.org/10.1007/s11367-016-1085-x>.
- Muteri, V., Cellura, M., Curto, D., Franzitta, V., Longo, S., Mistretta, M., Parisi, M.L., 2020. Review on life cycle assessment of solar photovoltaic panels. *Energies* (Basel) 13.
- Nassar, N.T., Graedel, T.E., Harper, E.M., 2015. By-product metals are technologically essential but have problematic supply. *Sci. Adv.* 1. <https://doi.org/10.1126/sciadv.1400180>.
- Nicoletti, G., Arcuri, N., Nicoletti, G., Bruno, R., 2015. A technical and environmental comparison between hydrogen and some fossil fuels. *Energy Convers. Manag.* 89, 205–213. <https://doi.org/10.1016/j.enconman.2014.09.057>.
- Norgate, T., Haque, N., 2010. Energy and greenhouse gas impacts of mining and mineral processing operations. *J. Clean. Prod.* 18, 266–274. <https://doi.org/10.1016/j.jclepro.2009.09.020>.
- Norgate, T., Haque, N., 2012. Using life cycle assessment to evaluate some environmental impacts of gold production. *J. Clean. Prod.* 29–30, 53–63. <https://doi.org/10.1016/j.jclepro.2012.01.042>.
- Norgate, T., Jahanshahi, S., 2011. Reducing the greenhouse gas footprint of primary metal production: where should the focus be? *Miner. Eng.* 24, 1563–1570. <https://doi.org/10.1016/j.mineng.2011.08.007>.
- Norgate, T.E., Jahanshahi, S., Rankin, W.J., 2007. Assessing the environmental impact of metal production processes. *J. Clean. Prod.* 15, 838–848. <https://doi.org/10.1016/j.jclepro.2006.06.018>.
- Nunez, P., Jones, S., 2016. Cradle to gate: life cycle impact of primary aluminium production. *Int. J. Life Cycle Assess.* 21, 1594–1604. <https://doi.org/10.1007/s11367-015-1003-7>.
- Nuss, P., Eckelman, M.J., 2014. Life cycle assessment of metals: a scientific synthesis. *PLoS ONE* 9. <https://doi.org/10.1371/journal.pone.0101298>.
- Pinto, R., Henriques, S.T., Brockway, P.E., Heun, M.K., Sousa, T., 2023. The rise and stall of world electricity efficiency: 1900–2017, results and insights for the renewables transition. *Energy* 269. <https://doi.org/10.1016/j.energy.2023.126775>.
- Qi, C., Ye, L., Ma, X., Yang, D., Hong, J., 2017. Life cycle assessment of the hydrometallurgical zinc production chain in China. *J. Clean. Prod.* 156, 451–458. <https://doi.org/10.1016/j.jclepro.2017.04.084>.
- Rachid, S., Taha, Y., Benzaazoua, M., 2023. Environmental evaluation of metals and minerals production based on a life cycle assessment approach: a systematic review. *Miner. Eng.* 198.
- REN21, 2022. *UNECE Renewable Energy Status Report. Paris2022*.
- Sanjuan-Delmás, D., Alvarenga, R.A.F., Lindblom, M., Kampmann, T.C., van Oers, L., Guinée, J.B., Dewulf, J., 2022. Environmental assessment of copper production in Europe: an LCA case study from Sweden conducted using two conventional software-database setups. *Int. J. Life Cycle Assess.* 27, 255–266. <https://doi.org/10.1007/s11367-021-02018-5>.
- Santero, N., Hendry, J., 2016. Harmonization of LCA methodologies for the metal and mining industry. *Int. J. Life Cycle Assess.* 21, 1543–1553. <https://doi.org/10.1007/s11367-015-1022-4>.
- Schenker, V., Oberschelp, C., Pfister, S., 2022. Regionalized life cycle assessment of present and future lithium production for Li-ion batteries. *Resour. Conserv. Recycl.* 187. <https://doi.org/10.1016/j.resconrec.2022.106611>.
- Schlömer, S., Bruckner, T., Fulton, L., Hertwich, E., McKinnon, A., Perczyk, D., Roy, J., Schaeffer, R., Sims, R., Smith, P., Edenhofer, O., Pichs-Madruga, R., Sokona, Y., Farahani, E., Kadner, S., Seyboth, K., Adler, A., Baum, I., Brunner, S., Eickemeier, P., Kriemann, B., Savolainen, J., Schlömer, C., von Stechow, C., Zwicker, T., Minx, J.C., et al., 2014. Annex III: technology-specific cost and performance parameters. *Climate Change 2014: Mitigation of Climate Change. Contribution of Working Group III to the Fifth Assessment Report of the Intergovernmental Panel on Climate Change*. Cambridge University Press, Cambridge, United Kingdom New York, NY, USA.
- Schrijvers, D.L., Loubet, P., Sonnemann, G., 2016. Developing a systematic framework for consistent allocation in LCA. *Int. J. Life Cycle Assess.* 21, 976–993.
- Sonderegger, T., Berger, M., Alvarenga, R., Bach, V., Cimprich, A., Dewulf, J., Frischknecht, R., Guinée, J., Helbig, C., Huppertz, T., et al., 2020. Mineral resources in life cycle impact assessment—part I: a critical review of existing methods. *Int. J. Life Cycle Assess.* 25, 784–797.
- Strezov, V., Zhou, X., Evans, T.J., 2021. Life cycle impact assessment of metal production industries in Australia. *Sci. Rep.* 11. <https://doi.org/10.1038/s41598-021-89567-9>.
- Torrubia, J., Valero, A., Valero, A., 2022a. Thermodynamic rarity assessment of mobile phone PCBs: a physical criticality indicator in times of shortage. *Entropy* 24. <https://doi.org/10.3390/e24010100>.
- Torrubia, J., Valero, A., Valero, A., 2022b. Beyond metal prices: geological scarcity as a physical cost allocation criterion. The case of rare earth element mining. In: *Proceedings of the ECOS 2022 35th International Conference on Efficiency, Cost, Optimization, Simulation and Environmental Impact of Energy Systems*. July 3, Copenhagen.
- Torrubia, J., Valero, A., Valero, A., Lejuez, A., 2023. Challenges and opportunities for the recovery of critical raw materials from electronic waste: the Spanish perspective. *Sustainability* 15, 1393. <https://doi.org/10.3390/su15021393>.
- Türkbay, T., Laratte, B., Çolak, A., Çoruh, S., Eleveli, B., 2022. Life cycle assessment of boron industry from mining to refined products. *Sustainability* (Switzerland) 14. <https://doi.org/10.3390/su14031787>.
- Tuusjärvi, M., Vuori, S., Mäenpää, I., 2012. Metal mining and environmental assessments: a new approach to allocation. *J. Ind. Ecol.* 16, 735–747. <https://doi.org/10.1111/j.1530-9290.2012.00469.x>.
- Ulrich, S., Trench, A., Hagemann, S., 2022. Gold mining greenhouse gas emissions, abatement measures, and the impact of a carbon price. *J. Clean. Prod.* 340. <https://doi.org/10.1016/j.jclepro.2022.130851>.
- Valero, A., Domínguez, A., Valero, A., 2015. Exergy cost allocation of by-products in the mining and metallurgical industry. *Resour. Conserv. Recycl.* 102, 128–142. <https://doi.org/10.1016/j.resconrec.2015.04.012>.
- Valero, A., Lozano, M.Á., Muñoz, M., 1986. A general theory of exergy saving. I. On the exergetic cost. *Computer-Aided Engineering and Energy Systems: Second Law Analysis And Modelling* 3, 1–8.
- Valero, A., Valero, A., 2014. *Thanatia, The Destiny of the Earth's Mineral Resources: A Cradle to Cradle Assessment*. World Scientific Publishing. ISBN 978-981-4273-93-0.
- van der Meide, M., Harpprecht, C., Northey, S., Yang, Y., Steubing, B., 2022. Effects of the energy transition on environmental impacts of cobalt supply: a prospective life cycle assessment study on future supply of cobalt. *J. Ind. Ecol.* 26, 1631–1645. <https://doi.org/10.1111/jiec.13258>.
- Van der Voet, E., Van Oers, L., Verboon, M., Kuipers, K., 2019. Environmental implications of future demand scenarios for metals: methodology and application to the case of seven major metals. *J. Ind. Ecol.* 23, 141–155. <https://doi.org/10.1111/jiec.12722>.
- Van Genderen, E., Wildnauer, M., Santero, N., Sidi, N., 2016. A global life cycle assessment for primary zinc production. *Int. J. Life Cycle Assess.* 21, 1580–1593. <https://doi.org/10.1007/s11367-016-1131-8>.
- Wei, W., Samuelsson, P.B., Tillander, A., Gyllenram, R., Jönsson, P.G., 2020. Energy consumption and greenhouse gas emissions of nickel products. *Energies* (Basel) 13. <https://doi.org/10.3390/en13215664>.
- song Yang, Y., Guo qi, Y., Zhu, W., Huang, J., 2019. Environmental impact assessment of China's primary aluminum based on life cycle assessment. In: *Transactions of Nonferrous Metals Society of China* (English Edition), 29, pp. 1784–1792. [https://doi.org/10.1016/S1003-6326\(19\)65086-7](https://doi.org/10.1016/S1003-6326(19)65086-7).
- Zhang, R., Ma, X., Shen, X., Zhai, Y., Zhang, T., Ji, C., Hong, J., 2020. Life cycle assessment of electrolytic manganese metal production. *J. Clean. Prod.* 253. <https://doi.org/10.1016/j.jclepro.2019.119951>.
- Zhang, T., Bai, Y., Shen, X., Zhai, Y., Ji, C., Ma, X., Hong, J., 2021. Cradle-to-gate life cycle assessment of cobalt sulfate production derived from a nickel–copper–cobalt mine in China. *Int. J. Life Cycle Assess.* <https://doi.org/10.1007/s11367-021-01925-x>.
- Zhang, Y., Sun, M., Hong, J., Han, X., He, J., Shi, W., Li, X., 2016. Environmental footprint of aluminum production in China. *J. Clean. Prod.* 133, 1242–1251. <https://doi.org/10.1016/j.jclepro.2016.04.137>.